

UDC 531.44

ABOUT THE INFLUENCE OF AUTOMOTIVE BRAKE PAD COMPOSITION ON FRICTIONAL PERFORMANCE. RESULTS OF NANO-SCALE MODELING

A. I. Dmitriev¹, W. Österle², H. Kloss²

¹Institute of Strength Physics and Materials Science SB RAS, Tomsk, Russia

²Federal Institute for Materials Research and Testing, Berlin, Germany

dmitr@ispms.tsc.ru

PACS 46.25.Cc, 68.35.Rh

The main problem in manufacturing friction materials is still a lack of sufficient information about the processes occurring in the surface layers of contacting bodies. This is due to the complexity of the processes which are taking place during friction and wear and by interdependency of mechanisms at various scale levels. This also may partly explain the complexity of structure of the composite materials which are used as brake pads, because a wide range of requirements have to be satisfied for modern braking systems. How variations of material composition affect the frictional characteristics of the friction pair is still an area of intense research. The present study used a computational method of the discrete approach — a method of movable cellular automata — to investigate the interaction of nano-scale features which are typical for the pad-disc-interface during automotive braking. The results can be useful for understanding the features of interaction of materials and control their performance properties.

Keywords: nanotribology, primary contacts, friction layer, modeling, movable cellular automata method.

1. Introduction

Since commercial brake pads usually are distinguished by very complicated formulations and the third body is formed by compaction of wear debris, its chemical composition usually is more complicated than the ones observed for the former applications [1,2]. In fact, third bodies produced during braking contain chemical elements from all ingredients of the pad formulation in addition to iron oxide from the cast iron brake disc mixed on a nanoscopic scale with grain sizes between 10 and approximately 100 nm depending on the type of ingredient. This can be seen most clearly by sampling wear particles emitted during a braking simulation in a test rig into size classes <1000 nm and subsequent investigation in an analytical transmission electron microscope (TEM) [3]. The same nanostructure was observed at the surfaces of pads and discs, proving that tribofilms are formed on both sides by compaction of wear debris. The films are discontinuous and usually about 100 nm thick. This finding inspired us to simulate the sliding behaviour of single asperity contacts covered by such friction layers with a granular computer model choosing a cell size of 10 nm, according to the smallest detected grain size of the experimentally observed nanostructure. In a recent review paper [4] we described friction and wear mechanisms taking place at different length scales during dry friction in automotive braking. The present paper will recapitulate the essentials for the simulation of smooth sliding conditions at a constant friction level with the method of movable cellular automata. Furthermore, an extension of the model will be presented by regarding more complicated material combinations in respect to type and size of automata, thus resembling more the real nanostructures observed experimentally.

Table 1. Parameters of model materials

	Young modulus E, GPa	Poisson ratio ν	Elastic limit σ_{y1} , MPa	Yield strength σ_{y2} , MPa	Ultimate tensile strength σ_s , MPa	Strain at σ_{y2} ϵ_{y2}	Breaking strain ϵ_s
Ferritic steel	206	0.28	450	500	550	0.04	0.106
Pearlitic steel	206	0.28	520	800	920	0.04	0.106
Iron oxide	380	0.3	290	305	340	0.008	0.009
Graphite	20	0.3	15	35	45	0.05	0.15
Copper	125	0.35	350	390	430	0.03	0.11
Soft copper	120	0.35	175	185	215	0.03	0.11
SiC	150	0.35	3000	4325	5000	0.06	0.18

2. MCA setup description

Theoretical investigation was carried out on the basis of modeling by the method of movable cellular automata (MCA). This choice was determined by the features of the MCA method to simulate such complicated processes as: mass mixing, damage generation and accumulation and so on. The formalism of the MCA method has already been described in [5]. The scheme of chosen two-dimensional setup is depicted in Fig. 1. It simulates a primary contact site according to Eriksson et al. [6], which is realized on the scale of the order of 1 micron. From pad site is a steel fibre as supporting substrate material. The supporting material on the disc side is pearlitic steel which is the matrix of cast iron. The free surfaces of both contacting bodies (first bodies) were covered with an oxide film consisting of nanoparticles of iron oxide and inclusions of solid lubricant. All previous simulations were based on the assumption that the solid lubricant had properties similar to graphite. Then we check the impact of substitution of graphite inclusions by soft nanoparticles of copper. All parameters of model materials are summarized in Table 1.

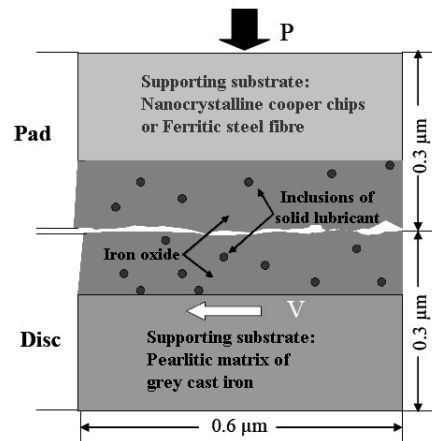


Fig. 1. Schematic presentation of the modelled pad-disc interface.

The following boundary conditions for modelling were used. A constant sliding velocity (V) equal to 10 m/s was applied on all particles of the bottom layer of the disc. At the same time their position in vertical direction was fixed. A constant normal force corresponding to the contact pressures in the range between $P = 15$ MPa and $P = 50$ MPa for different calculations was acted upon all the elements of the upper layer of pad. For both types of loading a linear procedure of value increasing was used with the following scheme. Initially the surfaces of pad and disc were separated. Then the loading with increasing velocity was applied on the particles of the bottom layer of the disc. Normal pressure was applied on the pad after all particles of

the disc (not only layer under loading) reach the maximum value of sliding velocity. Periodic boundary conditions were applied along the sliding direction. So, the number of particles was constant in the simulation, only redistribution of particles in the contact zone was studied. A surface profile with roughness on the nanometer scale was set deliberately prior to simulation. As shown previously, this setting exerts no major impact on the results of simulation [4,5]. The model calculates position and binding state of each automaton (particle) as well as resulting tangential forces or Coefficients of Friction (CoF) at the micro-contact for each time step.

3. Pressure dependency of a basic model structure

The main results of previous studies can be summarized as follows [4]: Neither metal-on-metal contacts nor oxide-on-oxide contacts provide stable friction conditions and a coefficient of friction (COF) around 0.4 which is desired for braking. A certain amount of soft inclusions within a rather soft but brittle oxide, like magnetite, is essential for achieving the desired properties. A prerequisite for smooth sliding behaviour is that a mechanically mixed granular layer (MML) is formed at the interface between the two first bodies. It has been shown that a volume fraction of at least 10 vol. % of soft nanoparticles (graphite in this case) is needed to form a MML irrespective of the applied pressure. Increasing the volume fraction of soft inclusions leads to a decrease of the COF. Since for braking we need smooth sliding, but a COF as high as possible, the fraction of soft particles should not be increased much beyond 10 vol %. A value of 13 vol % has proved to provide an optimum for both, smooth sliding and acceptable friction level. Although it would be most desirable for braking to have smooth sliding conditions and a COF irrespective of the applied pressure, a certain impact of pressure on structure formation and COF is unavoidable. This is demonstrated by Fig. 2 which shows the structures formed during simulation while applying different amounts of normal pressure. It can be seen clearly in Fig. 2 that, irrespective of applied pressure, there is always a zone of unlinked particles at the interface between the two third body layers (orange and green). This zone of unlinked particles originating from both third body films is the MML already mentioned at the beginning of this section. It is quite clear that the thickness of the MML depends on the applied pressure. This dependency is shown quantitatively in Fig. 3. The lowest pressure applicable in the model is 17.5 MPa for the structure with 13 % graphite and 7.5 MPa for a structure with 17.5 % graphite [4]. This is a quite large value compared to the nominal pressure in the range of 1-4 MPa which usually is applied during braking. We must keep in mind that we are considering micron-sized asperity contacts in the model. Therefore a factor of 10 compared to nominal pressure, which is related to the whole pad area, is reasonable. Furthermore, it should be mentioned that a constant sliding velocity of 10 m/s was maintained during modelling and that the time step of modelling of such nanostructures is of the order of 10^{-13} s, whereas the total time of one simulation was approximately 5×10^{-7} s.

The impact of pressure on MML-thickness does also affect COF-values which are calculated during modelling for each time step. This is shown in Fig. 4. The decrease of the COF-value with increasing pressure can be attributed to the increasing thickness of a quasi-fluid granular layer [7], which provides velocity accommodation between the fixed pad and rotating disc.

4. Effect of additional soft particles of larger size

Larger particles were defined as clusters of the basic nanoparticles with linked states to their neighbours. Soft copper as defined in [5] was selected as soft ingredient, because such species was observed experimentally in the third body of automotive brakes. Complete substitution of graphite nanoparticles with the copper clusters did not yield stable sliding conditions,

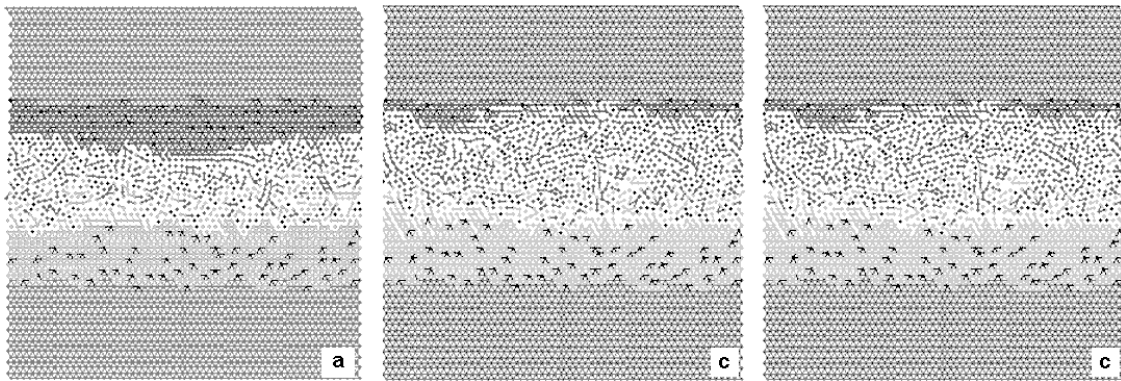


Fig. 2. Pressure dependency of the basic model structure after sliding simulations. The value of normal pressure: a) 17.5MPa; b) 26.3MPa; c) 30.0MPa.

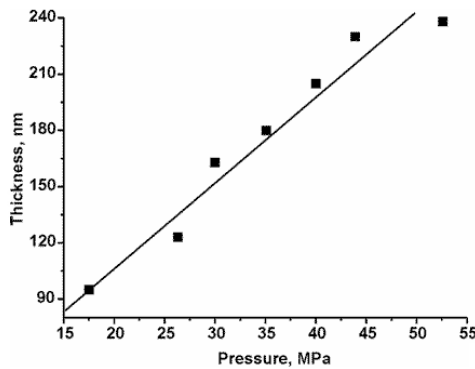


Fig. 3. MML-thickness of basic model structure as function of pressure

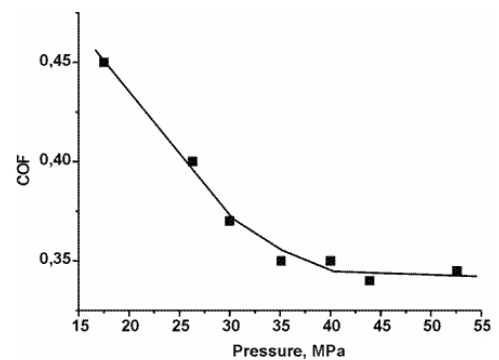


Fig. 4. COF of basic model structure as function of pressure

although breaking of links within the clusters and the release of single copper nanoparticles at the interface occurred during the simulation. But, since the soft particles were not distributed homogeneously in the third body, the formation of a mixed layer together with unlinked oxide particles did not take place.

On the other hand, if only half of the graphite particles of the basic structure were substituted by the copper clusters, a MML was formed and stable sliding conditions were achieved. This is shown in Fig. 5a and 5b, respectively. The copper clusters, still visible within the lower unaffected third body layer, are shown in magenta, and it is obvious that a MML has formed in which oxide, graphite and copper nanoparticles are distributed homogeneously. The corresponding COF-evolution during the simulation is shown by the black band and green curve in Fig. 5b, displaying momentary and averaged COF-values, respectively. A completely different behaviour was obtained with third body layers containing only 5 % graphite nano-inclusions without additional copper clusters. In this case no MML was formed (Fig. 6a) and COF-fluctuations between successive time steps remained high (Fig. 6b).

5. Effect of additional hard particles of larger size

The next step towards a more complicated nanostructure, albeit quite realistic with respect to experimental observations, is to introduce a certain amount of hard particles into the basic model structure. We selected SiC as hard particles because the stress-strain behaviour of this

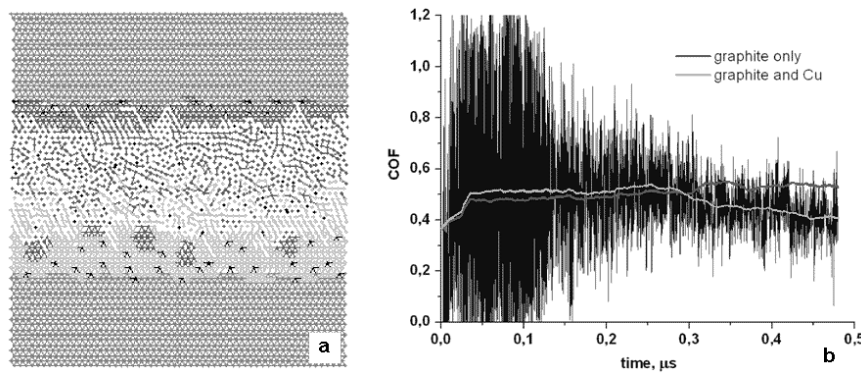


Fig. 5. a) Structure formation during sliding simulation for third body layers with 5.5 % graphite and 7.5 % coarse copper particles ($P=30$ MPa); b – Corresponding COF-evolution.

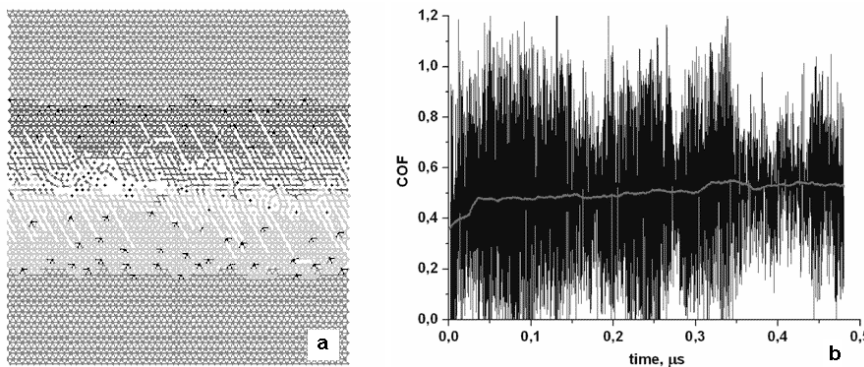


Fig. 6. a) Structure formation during sliding simulation for third body layers with 5.5 % graphite only ($P=30$ MPa); b – Corresponding COF-evolution.

material is well known from nanoindentation measurements not only at ambient but also at elevated temperatures [8]. Although SiC clusters were built in the same way as the copper clusters of the previous section, they behaved completely different during sliding simulation, as shown in Fig. 7. Because of the high mechanical strength of SiC, the bonds between adjacent nanoparticles within a SiC cluster (magenta colour) are not broken, while the oxide matrix, weakened by the graphite nanoparticles, forms the same granular layer as without SiC addition. Since a well developed MML with embedded SiC clusters was formed, smooth sliding with reduced COF fluctuations between adjacent time steps can be expected. This is shown in Fig. 8, where the scatter band of instantaneous COF-values corresponds to the structure with 4.8 % SiC. Similar results were obtained with 10 % SiC clusters. The coloured curves show average COF-values for the different model structures. A slight increase of the stationary COF-level while adding SiC clusters to the basic structure is revealed, but no significant difference between 4.8 and 10 % SiC is observed. Further simulations based on mechanical properties of SiC at elevated temperatures also did not change the results significantly (not shown here). This is because SiC is a hard material compared to magnetite even at 800°C. Fig. 9 provides an overview on the impacts of pressure and nanostructure on steady-state COF-values as determined by our model. Obviously, the pressure dependency of COF is not changed by adding hard particles, provided that these particles are small enough to be incorporated in the MML which forms during sliding simulation. Nevertheless the COF-level is increased over the whole range of applied pressures.

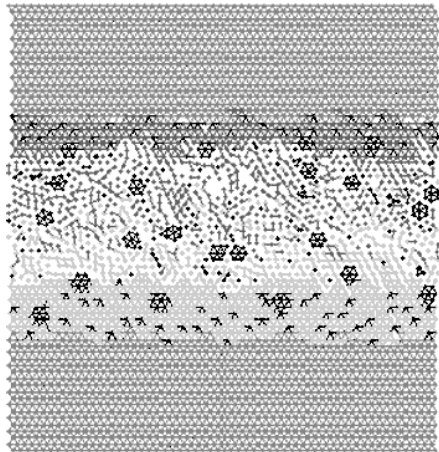


Fig. 7. Structure formation during sliding simulation for third body layers with 13 % graphite and additional coarse SiC particles ($p = 35$ MPa)

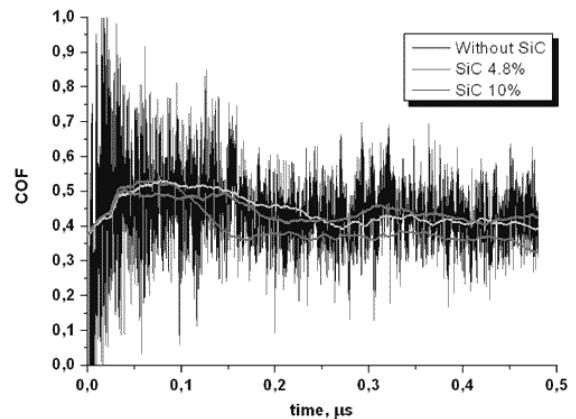


Fig. 8. COF-evolution of third body layers with 13 % graphite and additional coarse SiC particles ($p = 35$ MPa)

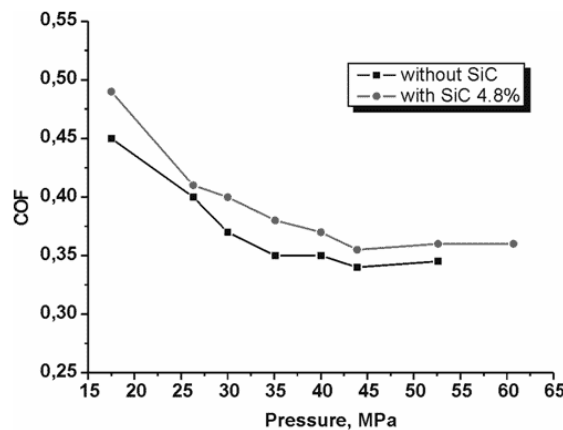


Fig. 9. Impact of SiC addition to pressure dependency of COF for friction layers with 13 % graphite

6. Conclusion

Owing to modelling, the role of solid lubricant inclusions in metal oxide based surface films can be assessed much better now. In particular, it has been shown that a homogeneous distribution of at least 10 vol % of soft nanoparticles is sufficient to provide smooth sliding conditions. Inhomogeneous distribution of the same amount of particles in the form of clusters would not be sufficient to initiate smooth sliding, but since the clusters are broken into their constituents easily, the number of effective nanoparticles will increase during tribological stressing, and, if the volume fraction is high enough, a solid lubricant film may form at the surface. Anyway, in the case of low volume fractions of the order of 10 %, a combination of single nanoparticles and clusters shows the same smoothing effect as a homogeneous distribution of the same volume fraction of single nano-inclusions. Thus we can conclude that as long as a certain amount of about 5 % of soft nano-inclusions is available, the size of additional solid lubricant additions is not relevant, but only its volume fraction. The additional solid lubricant constituent

will be crushed down to nanometric size and mixed with released oxide particles within the MML forming at the interface of the tribological couple. Thus one of the features which determine the COF of a micro-contact is the volume fraction of the soft ingredient in its third body layer. In respect to braking this finding is quite important because both types of solid lubricant inclusions i.e. graphite nanoparticles of 10 nm size and copper nanoparticles of 100 nm size were observed experimentally. Whereas soft constituents from first bodies will be transformed to nanoparticles easily, the same can not be expected for hard particles. In fact, this was revealed by the model as well. Although bonds between automata of the hard material forming clusters of hard particles are not broken, the bonds between elements at the cluster surface and adjacent third body matrix as well as within the third body itself are broken during sliding simulation, at least within a narrow zone at the interface. Thus a granular layer providing velocity accommodation can form, provided that the diameter of hard particle clusters is not larger as the MML-thickness. This scenario, revealed by modelling, correlates with experimental observations at third body layers of brakes which showed hard particles of various sizes.

Acknowledgements

Financial support for this work was obtained by German Research Foundation contract No. OS 77/18-1 and Russian Science Support Foundation, program of the specialized branches of RAS, project No. 13.13.3 and program No. 127 of SB RAS with exterior organization.

References

- [1] Rigney D.A., Hammerberg F.E. Unlubricated sliding behaviour of metals // *MRS Bull.*, 1998. P. 32–36.
- [2] Singer I.L. How third body processes affect friction and wear // *MRS Bull.*, June, 1998. P. 37–40.
- [3] Österle W., Bresch H., Dörfel I., Fink C., Giese A., Prietzel C., Seeger S., Walter J. Examination of airborne brake dust // In: *Proc. 6th European Conf. on Braking, JEF 2010, Lille, France, November, 24-25, 2010.* P. 55–60.
- [4] Dmitriev A.I., Österle W. Modeling of brake pad-disc interface with emphasis to dynamics and deformation of structures // *Tribol. Int.*, 2010. V. 43. P. 719–727.
- [5] Österle W., Prietzel C., Kloss H., Dmitriev A.I. On the role of copper in brake friction materials // *Tribol. Int.*, 2010. V. 43. P. 2317–2326.
- [6] Eriksson M., Bergmann F., Jacobson S. On the nature of tribological contact in automotive brakes // *Wear*, 2002. V. 252. P. 26–36.
- [7] Popov V.L., Psakhie S.G., Dmitriev A.I., Shilko E. Quasi-fluid nano-layers at the interface between rubbing bodies: Simulations by MCA // *Wear*, 2003. V. 254. P. 901–906.
- [8] Milman Y.V., Gridneva I.V., Golubenko A.A. Construction of stress-strain curves for brittle materials by indentation in a wide temperature range // *Science of Sintering*, 2007. V. 39. P. 67–75.